Polymer 50 (2009) 3329–3342

Contents lists available at ScienceDirect

Polymer

journal homepage: www.elsevier.com/locate/polymer

Morphology, structure and properties of conductive PS/CNT nanocomposite electrospun mat

Saeedeh Mazinani [a], Abdellah Ajji [b], Charles Dubois [a,*]

[a] CREPEC, Department of Chemical Engineering, Ecole Polytechnique of Montreal, P.O. Box 6079, Station Centre-Ville, Montreal, Quebec, Canada H3C 3A7
[b] CREPEC, Industrial Materials Institute, National Research Council Canada, 75, de Mortagne, Boucherville, Quebec, Canada J4B 6Y4

ARTICLE INFO

Article history:
Received 13 January 2009
Received in revised form
3 April 2009
Accepted 11 April 2009
Available online 9 May 2009

Keywords:
Nanocomposite electrospun fibers
Carbon nanotube
Polystyrene

ABSTRACT

The morphologies and properties of Polystyrene (PS)/Carbon Nanotube (CNT) conductive electrospun mat were studied in this paper. Nanocomposite fibers were obtained through electrospinning of PS/Di-Methyl Formamide (DMF) solution containing different concentrations and types of CNTs. The dispersion condition of CNTs was correlated to morphologies and properties of nanocomposite fibers. A copolymer as an interfacial agent (SBS, Styrene–butadiene–styrene type) was used to modify the dispersion of CNTs in PS solution before electrospinning. The results showed that the presence of the copolymer significantly enhances CNT dispersion. The fiber diameters varied between 200 nm and 800 nm depending on CNT type, polymer concentration and copolymer. The final morphological study of the fibers showed that CNT addition caused a decrease in beads formation along fiber axis before percolation threshold. However, addition of CNTs above percolation increased the beads formation, depending on the dispersion condition. The presence of SBS modified the dispersion, reduced the fiber diameter and the number of bead structures. Electrical conductivity measurements on nanocomposite mats of 15–300 μm in thickness showed an electrical percolation threshold around 4 wt% MWCNT; while the samples containing SBS showed higher values of conductivities below percolation compared to the samples with no compatibilizer. Enhancement in mechanical properties was observed by the addition of CNTs at concentrations below percolation.

1. Introduction

The electrospraying process was discovered by Formhal and disclosed in patent literature in 1934. Since then, this process has found a great deal of interests in spite of its simplicity [1]. Electrospinning is the most frequently used method to produce fibers of nanometric size. This process was known as electrostatic spraying before 1993, and there were only a few publications employing this technique [2]. Reneker and Chun revived this technology in the 1990s and they showed the possibility of employing this process for different kinds of polymer solutions in 1996 [3]. In this process, a syringe pump moves the solution out of the spinneret at a constant and controllable rate. Application of a high voltage difference between the syringe tip and a target screen for collection induces electric charges that are distributed over the surface of droplet, which is finally attracted to the other side due to the high electric field and forms drops, fibers or beaded fibers. Various types of nanoparticles dispersed in polymer solutions have been embedded recently in nanofibers through this process to modify the final properties of electrospun fibers. Among them, carbon nanotubes have attracted a great attention. In fact, rapidly after CNT development [4], this nanoparticle has been widely used to enhance electrical or mechanical properties of electrospun polymer fibers to various extents [5–8].

Ra et al. electrospun PAN/MWCNT nanofibers and showed that there is an electrical anisotropy in final nanofibers along fiber axis compared to fiber cross section [6]. They showed that nanofibers' diameter is strongly dependant on CNT concentration. An increase in the amount of CNT enhances the conductivity of the polymer solution and produces a larger electrical current during electrospinning. The addition of charge accumulation overcomes cohesive force and intensifies repulsive forces and fibers of smaller diameter are formed [6]. CNT composite nanofibers were produced using PVDF as the matrix by Seoul et al. [7]. They found that there were different values of percolation threshold which were 0.003 wt% CNT for CNT/PVDF/DMF solution, 0.015 wt% for spin coated film of the same material and 0.04 wt% for electrospun nanofiber mat. PMMA was employed as the matrix for CNT composite nanofiber manufacturing, in 2004, by Sung et al. [8]. They embedded different concentrations of CNTs from 1 to 5 wt% by the use of in-situ bulk

* Corresponding author. Tel.: +1 514 340 4711x4893; fax: +1 514 340 4159.
E-mail address: charles.dubois@polymtl.ca (C. Dubois).

0032-3861/$ – see front matter © 2009 Elsevier Ltd. All rights reserved.
doi:10.1016/j.polymer.2009.04.070

polymerization. However, they detected a reduction in electrical conductivity by this method in comparison with a solution dispersion process. They showed that existence of pore structures and wrapping of PMMA polymer chains around the CNTs are the main causes of electrical conductivity reduction compared to solution mixing method [8]. Enhancement of CNT dispersion and its effect on electrospun fiber morphologies and properties is one of the main aims in this work. We intend to use compatibilization methods rather than chemical modification to improve CNT dispersion and maximize electrical properties. There are several papers related to the use of CNTs as fillers along with dispersion modification techniques employed in electrospinning process [9–11]. New types of block copolymers have recently been introduced for CNT dispersion modification, especially above electrical percolation. The structures, properties and the method of functionalities of these specific copolymers have been proved both theoretically and experimentally [12–14].

Other studies investigated the structure and properties of PS electrospun nanofibers from different points of view. The earliest among them studied the effect of solvent on final fiber morphologies and fiber surface has been studied. In particular, there is a large number of papers about controlling bead morphology along fiber axis and final fiber morphologies [15–22]. Lin et al. studied the effect of cationic and non-ionic surfactants [23] on bead morphology and fiber surface. In 2005, Shenoy and his colleagues investigated the effect of chain entanglements on various polymer solutions for electrospinning, including polystyrene solutions [24]. They proved the considerable effect of molecular weight and polymer concentration on electrospun fiber formation. They showed that, depending on polymer concentration and chain entanglements, there are different regions in which changes in morphology from beaded to smooth fiber occur [24]. In 2006, the change in bead and fiber morphology and also the fiber diameter during electrospinning of polystyrene was studied by Eda et al. [25,26]. They showed that a change in molecular weight or concentration affects final morphology even though $[\eta]c$ would be kept constant. In another work, they observed that solidification and instability of electrospun fibers could occur at different distances from the capillary, depending on the rheological condition of solution [27]. In one of the most recent works on PS nanofibers production, Wang et al. [28] could obtain scaling laws between the fiber final structure and process variables.

There are only few studies focusing on PS/CNT electrospun nanofibers. Sen et al. studied the effect of SWCNT addition to PS as well as to polyurethane (PU). They obtained oriented CNT inside PS nanofiber and some other polymeric materials [29], as evidenced from TEM images. In 2006, Ji and his colleagues used carboxyl-functionalized MWCNT inside PS and showed that the particles arranged quite well along the fiber axis [30]. Pan et al. produced polyelectrolyte hollow nanofibers out of PS/MWCNT solution mixture [31]. In this work, PS/MWCNT electrospun nanofibers were used as templates for self-assembly of polyelectrolytes [31]. In one of the most recent works in the field of electrospinning and CNT nanocomposite fiber manufacturing, Sundaray and his coworkers studied the properties of a single nanofiber of PS/MWCNT [32]. They investigated the morphology and electrical conductivity of a single nanofiber containing low amount of MWCNT. They obtained a low percolation threshold (0.05% w/w) for only a single electrospun fiber. In their work, they could improve conductivity to 10^{-6} S/cm after percolation [32].

The review of previous work on electrospun CNT filled polymeric fibers shows that several aspects of the materials/process used in their preparation required further study. The final properties of electrospun mat composed of nanocomposite nanofibers including different types of CNTs are one point of interest. In addition, dispersion modification employing coupling agent and studying its effect on final electrical and mechanical properties is also of considerable interest. Different techniques such as rheometry and viscometry could be employed to perform the effect of adding CNT and studying the effect of dispersion on final morphology and properties. Electrospun polymer/CNT nanofibers and their properties as final conductive non-woven mat were not studied in details so far. Moreover, the properties of PS/CNT at different CNT concentrations are yet to be characterized. The final properties of electrospun PS/CNT as a conductive mat especially at more concentrated levels of CNTs were not shown in any previous works.

In the present study, polystyrene solutions containing different types and concentrations of carbon nanotubes (single-wall, double-wall and multi-wall) are electrospun to produce nanocomposite fibers. The effect of CNT addition on final morphologies of fibers is studied both quantitatively and qualitatively. We mainly focus on final nanofibers and mats characteristics at a wide range of MWCNT concentration and especially at high concentrations of different types of CNTs. Electrical conductivity of electrospun mats composed of PS/CNT nanofibers is evaluated here for the first time. Dispersion of CNT in initial electrospinning solution is studied in detail using rheological and optical techniques. The use of an SBS type copolymer to improve the dispersion of MWCNT in PS solution is, to the best of our knowledge, reported for the first time in this work. In addition, electrical properties and mechanical characteristics of resulting electrospun mats at different CNT contents and types are obtained.

2. Experimental

2.1. Polymer solution preparation

The polymer used in this work was an extrusion grade polystyrene (168M, BASF Co.), dissolved at 20% w/w concentration in dimethyl formamide (DMF) (good solvent for PS as well as CNT dispersion); the solvent was purchased from Aldrich Co. Carbon nanotubes employed in this work were produced by a chemical vapor deposition process (CVD) and purchased from Helix Co., USA. Single-wall carbon nanotubes (SWCNT) and double-wall carbon nanotubes (DWCNT) with purities of 90% and multi-wall carbon nanotubes (MWCNT) with purity of 95% were used in this investigation as nanoparticles to improve the conductivity. The nominal diameter range of SWCNT, DWCNT and MWCNT was respectively of 1.3 nm, 4 nm and 10–100 nm. All three types of CNT had length in range of 0.5–40 μm (Fig. 1).

CNTs at different concentrations were dispersed mechanically in the polymer solution by a 4-h sonication treatment at room temperature followed by continuous mechanical mixing before electrospinning. No surface modification technique was employed in this work in order to prevent the detrimental effect that these treatments can have on the conductivity of the CNT. TEM results after 4 h sonication in pure methanol at different positions along CNT bundles show no obvious change in CNT length (Fig. 1). Styrene–Butadiene–Styrene (SBS-Kraton; G-1647), copolymer was used to improve the dispersion of CNTs in the solutions and electrospun fibers and to study the effect of copolymer addition. Following the proposed method for CNT dispersion modification [14], the copolymer was used in equal amounts of CNT for enhancing their dispersion at different concentrations.

2.2. Electrospinning process

The electrospinning set-up employed in this work consisted of a high voltage power supply (Gamma Inc.), a syringe pump to

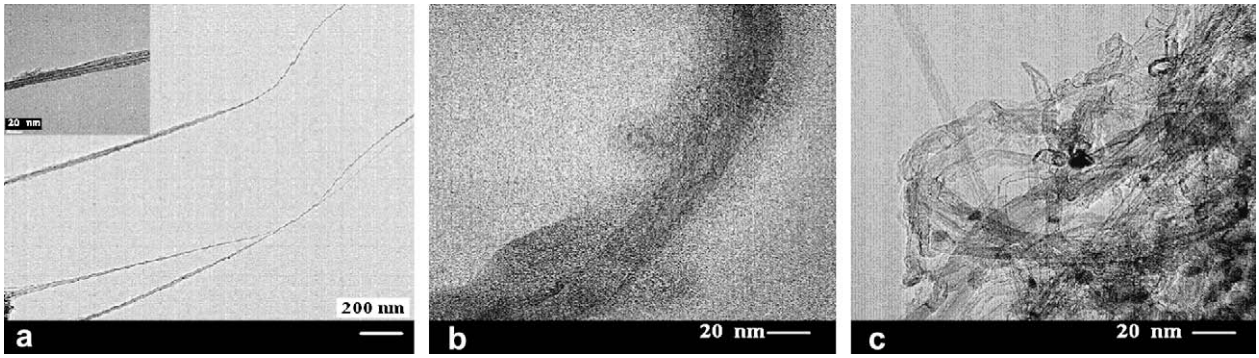

Fig. 1. Transmission electron Microscopy (TEM) images of CNTs utilized in this work after sonication. a) Multi-wall Carbon Nanotube; b) Double-wall Carbon Nanotube; c) Single-wall Carbon Nanotube; TEM (JEOL, JEM-2100 F).

deliver the solution at specific flow rates (PHD 4400, Harvard Apparatus), a syringe connected to a stainless steel needle (22 gauge, Popper & Sons Inc.), and finally a stainless steel collecting drum (15 cm diameter). Fiber mats were collected in both static and rotating drums, based on the requirements of specific samples for different experiments. An average electrical potential difference of 25 kV was employed for all types of materials. The voltage was imposed on the needle, positioned at a 15 cm distance from the collector and a volumetric flow rate of 0.8 mL/h was imposed. All experiments were conducted at ambient pressure, temperature and average relative humidity of 20%. A summary of different carbon nanotube concentrations and types studied here and the resulting fiber diameter and morphology are given in Table 1.

2.3. Initial material characterization

The effect of CNT on viscosity of the solutions was studied as it represents one of the key properties that may affect the electrospinning process. We used Cannon-Fenske-Routine (CFR) viscometers to characterize the change in viscosity with CNT addition. In addition we used a Bohlin CVO 120 stress-controlled rheometer to evaluate the rheological properties of initial polymer solution.

Optical microscopy observations of initial solutions containing CNTs at the same dispersion condition were used in parallel with viscometry to evaluate the dispersion condition of solutions containing carbon nanotubes at different concentrations.

The conductivity of the solutions at different carbon nanotube concentrations was measured using an accumet AP85 conductivity meter by Fisher Scientific. All the measurements were performed after mixing and before electrospinning.

2.4. Morphological characteristics and final properties

Raman spectroscopy technique was used for CNT detection in final non-woven mat. Raman spectra were recorded on a Renishaw spectrometer equipped with an inVia Raman microscope. The samples were tested using a NIR laser (785 nm) with a grating of 1200 g/mm in the regular mode and the microscope magnification used was 20×.

A Hitachi S-4700 scanning electron microscopy (SEM) was used on platinum coated samples to characterize the final morphologies of fibers at different processing conditions. An optical microscope, Dialux 20 (Leitz,WETZLAR), was employed to check and analyze the dispersion condition and position of CNTs inside fibers. This method was used to detect CNT positions along with dispersion conditions and morphological characteristics.

The electrical conductivity of final electrospun mats was measured to assess the effect of CNT on nanofibers. For this purpose, a two-probe technique was employed, using a combined set-up of KEITHLEY 6620 as a current source and Agilent 34401 A (6½ Digit Multimeter) as voltage source.

The mechanical properties of selected samples produced at different processing conditions were obtained from a microtester 5548 (Instron Inc.) All the experiments were conducted on strips of 5 mm in width and 15 mm in length cut from electrospun samples. The samples included different ranges of thicknesses from 50 to 300 μm. A load cell of 5 N and stretch speed of 10 mm/min were the

Table 1
Summary of nanocomposite nanofibers obtained and the resulting fibers characteristics.

Polystyrene concentration (% w/v)	CNT type	CNT concentration (%)	Resulting morphology	Range of nanofiber diameter (nm)
20	–	0	High concentration of beads on fibers	400–1500
20	MWCNT	0.5; 1; 2; 3; 4; 5; 7	**1%:** Smooth fibers **Other concentrations**: Bead/Fiber morphology; beads depend on CNT concentrations Less beads compared to pure PS electrospun fibers	300–1100
20	MWCNT modified with Copolymer	1; 2; 3; 4; 5	**1% & 2%:** Smooth fibers **Other concentrations**: Bead/Fiber morphology; beads depend on CNT/Copolymer concentrations Less beads compared to the fibers obtained form pure MWCNT/PS nanofibers	200–700
20	SWCNT	1; 5	Bead/Fiber morphology; More beads formation at higher concentration (5%)	100–1400
20	DWCNT	1; 5	Bead/Fiber morphology; More beads formation at higher concentration (5%)	150–1200

Table 2
Relative viscosity of solutions ($\eta/\eta_{solvent}$) at different CNT types and concentrations.

CNT Type	CNT concentration (%)						
	0	0.5	1	2	3	4	5
MWCNT	160.5 ± 1.0	92 ± 2.7	95.25 ± 1.7	96.8 ± 2.6	121.8 ± 4.6	129 ± 4.7	130 ± 1.4
MWCNT/copolymer	160.5 ± 1.0	93.2 ± 1	98 ± 1.4	114.5 ± 2.4	145.8 ± 1.7	274.5 ± 1.7	451.3 ± 41.6
SWCNT	160.5 ± 1.0	–	112.2 ± 4.3	–	–	–	–
DWCNT	160.5 ± 1.0	–	118.5 ± 0.6	–	–	–	–

best testing conditions for mechanical characterization of the electrospun samples.

3. Results and discussions

3.1. Initial material characterization

Various characteristic parameters of the initial solution will determine the final fiber structure and diameter. Among them, surface tension, solution conductivity and viscosity are the most important determining factors. In this work, we mainly focused on the effect of dispersion of CNTs and the suspension viscosity and conductivity on the electrospinning process.

The measurement of viscosity was conducted at different CNT concentrations for samples containing different types of CNTs, with and without copolymer. The results obtained show that the viscosity decreases considerably with addition of CNTs (Table 2). The reduction of viscosity is observed in all samples containing CNTs. This could be because of polymer chains break-up during sonication. The reduction in molecular weight causes the viscosity of samples containing CNTs decrease compared to pure PS solution. Addition of MWCNTs, even at 5% concentrations, shows the decreasing viscosity of MWCNT/PS solutions compared to pure PS solution. A comparison of the results at 0.5, 1 and 2% MWCNT shows that addition of MWCNT does not change viscosity with MWCNT concentrations but MWCNTs affect considerably the viscosity of the polystyrene solution above 3%. Below 3% MWCNTs, solutions with MWCNTs are stable for long period of time, no large agglomerates are found (Table 2). Above 3% MWCNT, viscosity of initial solution considerably increases and MWCNTs suspension in solutions are mostly unstable. The results prove that there is a network formation and structure build-up between 2% and 3% for this system. We also studied samples containing a SBS copolymer and MWCNT and a similar result was obtained. In prepared solutions, addition of MWCNT decreases the viscosity of solution (Table 2). However, viscosity increases at 3% MWCNT/Copolymer concentration which shows the region of percolation in this system. The viscosity measured for sample with 2% and 3% MWCNT and copolymer is higher than for samples containing 2% and 3% pure CNT, which could be an evidence of SBS existence along with the dispersed MWCNTs. Copolymer chain interactions with CNTs cause an increase in suspensions viscosity; but they still remain less viscous than original PS solutions. Addition of high molecular weight SBS causes gradual increasing of viscosity. This effect is even more obvious at high concentrations of MWCNT and copolymer (Table 2). Therefore, using viscosity as evidence can only be inconsistent with similar systems, since adding copolymer changes the properties of system and viscosity accordingly. The effect of CNT addition on viscosity at 1% concentration of SWCNT, DWCNT and MWCNT is also assessed.

MWCNT is much easier to disperse, and therefore, sample containing 1% MWCNT shows the lowest viscosity in spite of larger size of MWCNTs. Therefore, samples with 1% SWCNT and DWCNT show higher viscosities compared to 1% MWCNT and 1% MWCNT/copolymer samples. SWCNT and DWCNT are smaller in size; however, their poor dispersion increases the viscosity of their solutions compared to MWCNT [33,34]. Viscosity in solutions with MWCNT/copolymer is not different from that with only MWCNT and is lower than that for those containing SWCNT and DWCNT. This could be due to the finer particle size (agglomerates) in solutions with both MWCNT and copolymer and better dispersion quality (Table 2). The results obtained show that viscometry could be an indirect mean of evaluating the quality of particles dispersion in the solution. The lower the viscosity, the more the compatibility is between particles and solution and better is the quality of the dispersion. Moreover, it could be used as a criterion for obtaining the system network formation concentration. Below 3% MWCNT, no network structure is formed to cause an increase in the viscosity of the solutions. Even though, despite of high shear rate flow fields in viscosimetry, no network structure could be observed coming from CNT particles, there is still considerable difference in viscosities before and after percolation.

The viscosity of the system was studied at different concentrations of MWCNTs below percolation at low range of shear rate (Fig. 2). We used this technique to evaluate the reliability of the results obtained from viscometry technique.

The tests were done at room temperature and constant stress of 20 Pa. The system shows totally Newtonian behavior; however, the reduction of viscosity by molecules break-up is not distinguishable at low frequencies. It shows that in high shear flow field, the difference in viscosities of pure sample with the ones containing CNT is more obvious (Table 2 & Fig. 2). This could be because of the sliding effect of CNTs in addition to molecular weight reduction in the samples containing CNT. The results in Fig. 2 could show that the samples containing 2% MWCNT have no network formation inside as obtained previously by viscometry technique (Table 2).

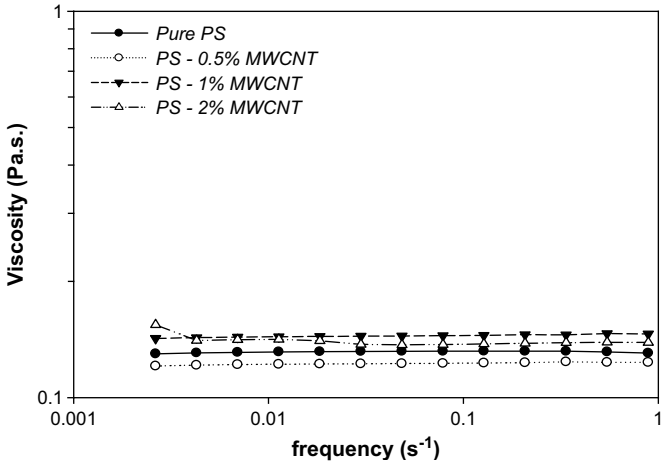

Fig. 2. Viscosity vs. frequency at different MWCNT concentrations below rheological percolation threshold (CVO 120, Room temperature, at 20 Pa constant stress).

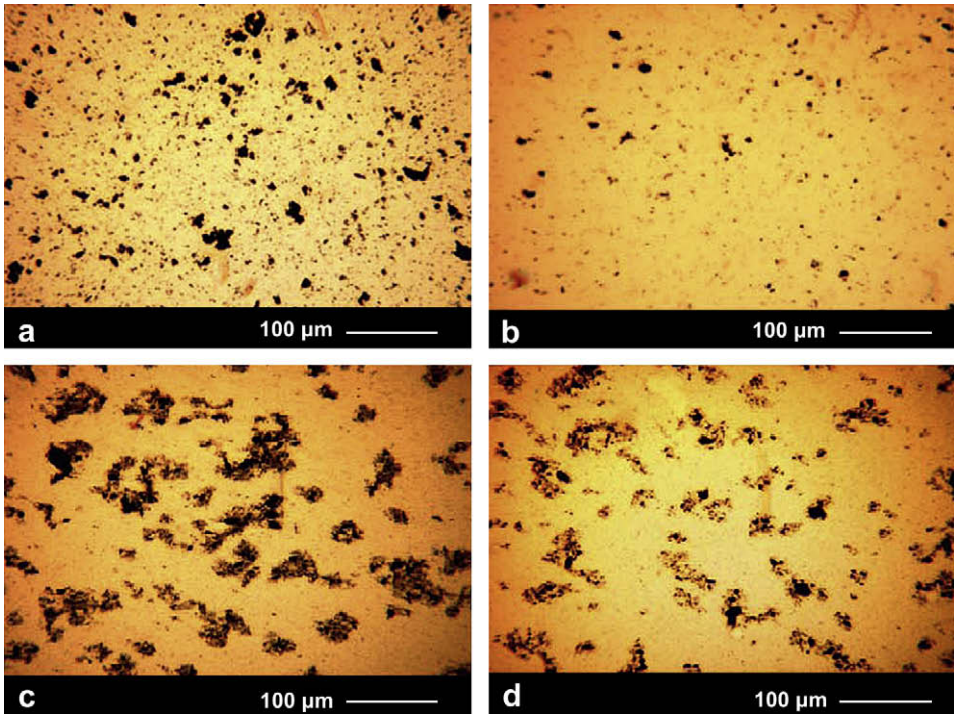

Fig. 3. Optical microscopy on dispersion condition of initial solution below rheological percolation (1% MWCNT) and above percolation (4% MWCNT) with and without copolymer. a) 1% MWCNT; b) 1% MWCNT & copolymer; c) 4% MWCNT; d) 4% MWCNT & copolymer.

Optical microcopy was also used to evaluate the dispersion condition of CNTs in the initial polymer solution. This technique had the advantage of no limitations in terms of CNT concentration compared to viscosimetry and was very useful in this work. Fig. 3 shows the change of particle sizes both below rheological percolation (1% MWCNT) and above percolation (4% MWCNT).

As shown, upon addition of more and more MWCNT, it becomes more difficult to disperse the nanoparticles and large agglomerates are formed. The effect of copolymer addition on the dispersion quality is shown in Fig. 3. At 1% concentration (Fig. 3a and b), addition of copolymer causes a reduction in agglomerated particles size and fewer particles can be observed by optical microscopy. Above percolation and at 4% (Fig. 3c and d), the copolymer presence reduced particles size and allowed formation of an interconnected network structure, and thus MWCNTs are better dispersed with much less agglomerates (Fig. 3c and d).

The dispersion state of different PS/CNT solutions has been studied by optical microscopy at 5% concentration of different CNTs (Fig. 4).

The optical images confirm the results from viscometry. SWCNT and DWCNT show the largest sizes of CNT agglomerates and therefore, they induce a higher viscosity below percolation (Fig. 4a and b). In contrast, MWCNT showed smaller and less agglomerates (Fig. 4c). Copolymer addition in the latter case even induced particle size reduction compared to MWCNT suspensions without copolymer (Fig. 4d).

The results obtained from viscosimetry prove that at 1% concentrations of different carbon nanotubes (Table 2), the solutions are all below the concentration for network formation. Even though, there is a slight difference of suspension viscosity amongst different carbon nanotube types, it is not significant enough to be an evidence for structure build-up. The increase in the viscosity in the case of SWCNT and DWCNT is because of poor dispersion condition of carbon nanotubes. Moreover, the results from optical microscopy at 5% (Fig. 4) along with viscometry (Table 2) could be a proof that the system is above the concentration for network formation at 5% of different carbon nanotubes types. In this study, we mainly compare the results from 1% of different carbon nanotube types which is below network formation as described above (Table 2). In addition, 5% concentration of carbon nanotubes is chosen as a concentration above network formation.

The results obtained from electrical conductivity measurements of solutions containing various concentrations of MWCNT are given in Table 3. As expected, addition of MWCNT causes an increase of the initial solution conductivity.

Comparing the results obtained from different types of carbon nanotubes shows that SWCNT containing solutions are more conductive; 54 μS/cm at 1% SWCNT concentration compared to 20 μS/cm at 1% MWCNT concentration. Moreover, addition of copolymer causes a decrease in the amount of conductivity; 79 μS/cm at 5% MWCNT/copolymer concentration compared to 88 μS/cm at 5% MWCNT concentration. The reduction in conductivity by adding copolymer might be due to partial coating of the carbon nanotubes by the copolymer coupling agent. The results show that addition of carbon nanotube enhances the conductivity of the system, which could be an important determining factor on final morphology.

3.2. Raman spectroscopy

Raman spectra of non-woven mats obtained from different types of carbon nanotubes/PS nanofibers are shown in Fig. 5. Among the characteristic peaks of multi-wall carbon nanotubes detected by Raman spectroscopy, three peaks could be distinguished. Two string peaks are located at 1580 cm^{-1} (G), and 1350 cm^{-1} (D) and a weak peak is also detected at around 2700 cm^{-1} (G′) [35,36].

The intensity and ratio of these peaks (D/G ratio) vary depending on carbon nanotube type and surface structure. The peaks related to SWCNT and DWCNT show more similar structure as expected; however SWCNT and DWCNT are fundamentally different from MWCNT characteristic peaks (D/G ratio).

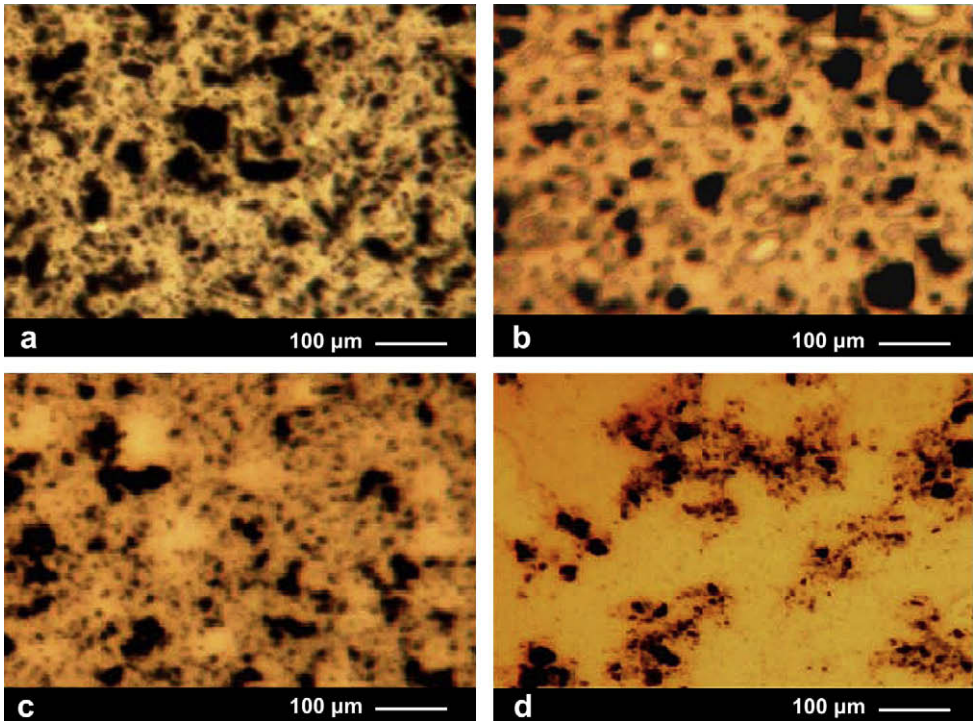

Fig. 4. Optical microscopy on dispersion condition of initial solution. a) 5% SWCNT; b) 5% DWCNT; c) 5% MWCNT; d) 5% MWCNT & Copolymer.

3.3. Morphology of electrospun fibers and mats

In this work, two methods were chosen to characterize the final morphologies of fibers. First, the fiber morphologies were analyzed qualitatively through SEM, followed by some quantitative image analysis. Second, optical microscopy was used to detect CNT localizations inside the fibers. Moreover, this technique was also used to evaluate the effect of copolymer addition on final dispersion condition of CNTs inside the fibers.

The final morphologies of the fibers are dependant on several characteristics of the initial solution such as viscosity, surface tension and conductivity in addition to some process and environmental conditions (temperature and humidity). The latter were not changed for this study and only the effect of material parameters was assessed, by changing the types and concentrations of CNTs.

Fig. 6 shows the effect of MWCNT addition at different concentrations on final fibers morphologies. As it is depicted in the results, electrospun PS fibers without MWCNTs are mixtures of beads and fibers at 20% PS concentration (Fig. 6a). Addition of MWCNTs to the PS solution causes a gradual decrease in the relative number of bead structures among the fibers. This effect is explained by our previous observation that the addition of MWCNTs increases the solution conductivity and decreases the solution viscosity under high shear rates flow conditions; which are also found in the electrospinning process while solution is moving through syringe before exit. The value of shear rate for the viscometer we have used is in the range of 1–80 s^{-1}. In the electrospinning set-up we can estimate an average shear rate of about 4 s^{-1}, resulting from a 0.8 mL/h volumetric flow rate through a PS22 gauge.. The best condition for smooth, beadless fiber production is below a 2% concentration of MWCNT (at 1%, beads are even less) (Fig. 6c and d). At 3% and 4% MWCNT and after rheological percolation (Above 3% MWCNT), the amount of bead structures in samples containing different concentrations of MWCNTs is almost the same (Fig. 6e and f). However, at two higher concentrations, 5% and 7% of MWCNT, there is again an increase in the amount of bead structures along fiber axis (Fig. 6g and h). The fibers at higher concentrations had smaller diameters and more beads in their structures compared to lower concentrations of MWCNTs. Followed by the decrease in fiber diameter, the sizes of beads along fiber axis are decreased correspondingly. Therefore, at higher concentrations smaller beads are shaped along fiber axis. The small beads are more obvious in the next optical microscopy test results by dark aggregate formation which will be discussed in more detailed.

Table 3
PS/CNT solutions conductivity (μS/cm) at different MWCNT concentrations.

Concentration (%)	0	1	3	5
MWCNT	1.2	20.3	34.5	88.2

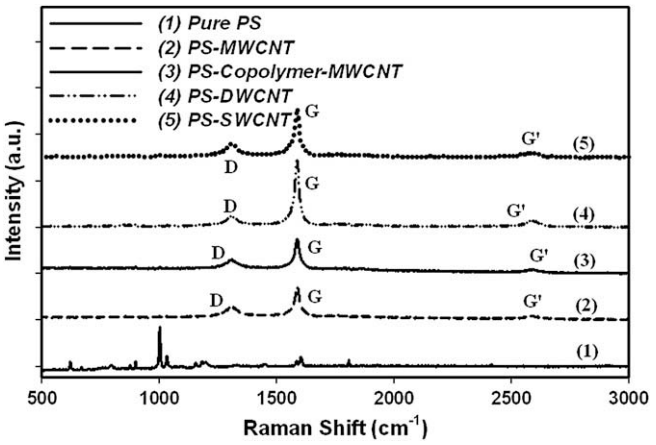

Fig. 5. Raman spectra of final non-woven mat containing different types of carbon nanotubes.

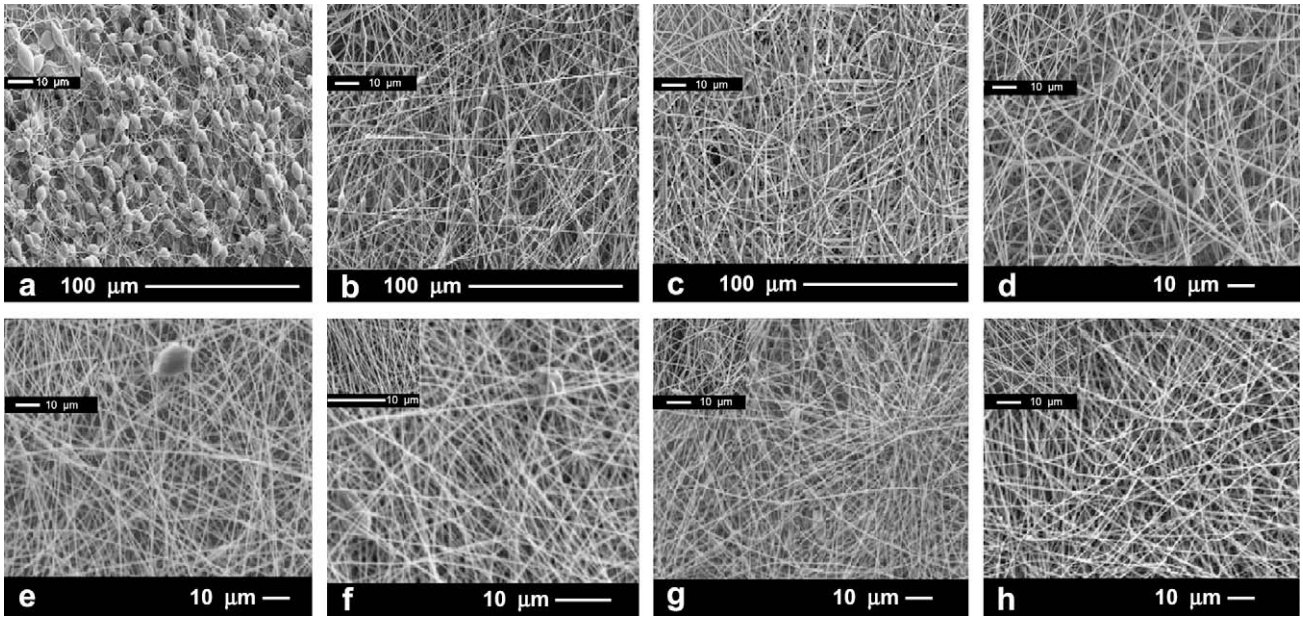

Fig. 6. SEM photos of PS (20%)/MWCNT at different CNT concentrations. a) Pure PS; b) 0.5% MWCNT; c) 1% MWCNT; d) 2% MWCNT; e) 3% MWCNT; f) 4% MWCNT; g) 5% MWCNT; h) 7% MWCNT.

The quantitative analysis shows that the fiber diameter reduces as CNT content increases in initial solution up to 4–5% (Fig. 7). At 4–5% and 7% MWCNT concentration, the value of fiber diameter is optimized and has the least value. The histograms of fiber diameter distribution show that, for all concentrations, a wide distribution of fiber diameters is obtained.

In the case of MWCNT addition combined with copolymer almost the same morphological trend as discussed above is observed (Fig. 8). The smoothest fibers are obtained at 1% and 2% concentrations of MWCNT/copolymer; while bead structures content increases by addition of CNTs to 5% MWCNT/copolymer. A comparison of the morphologies of systems with copolymer and without copolymer shows that addition of copolymer causes a decrease in the amount of bead structures compared to the system with pure MWCNT, for all concentrations.

Histograms of MWCNT/copolymer electrospun fiber show similar trends as samples with pure MWCNT (Fig. 9). The addition of MWCNT causes fiber diameter reduction and 4% MWCNT/Copolymer concentration is the optimum value. Fiber diameters decrease considerably by the addition of 1% MWCNT/copolymer.

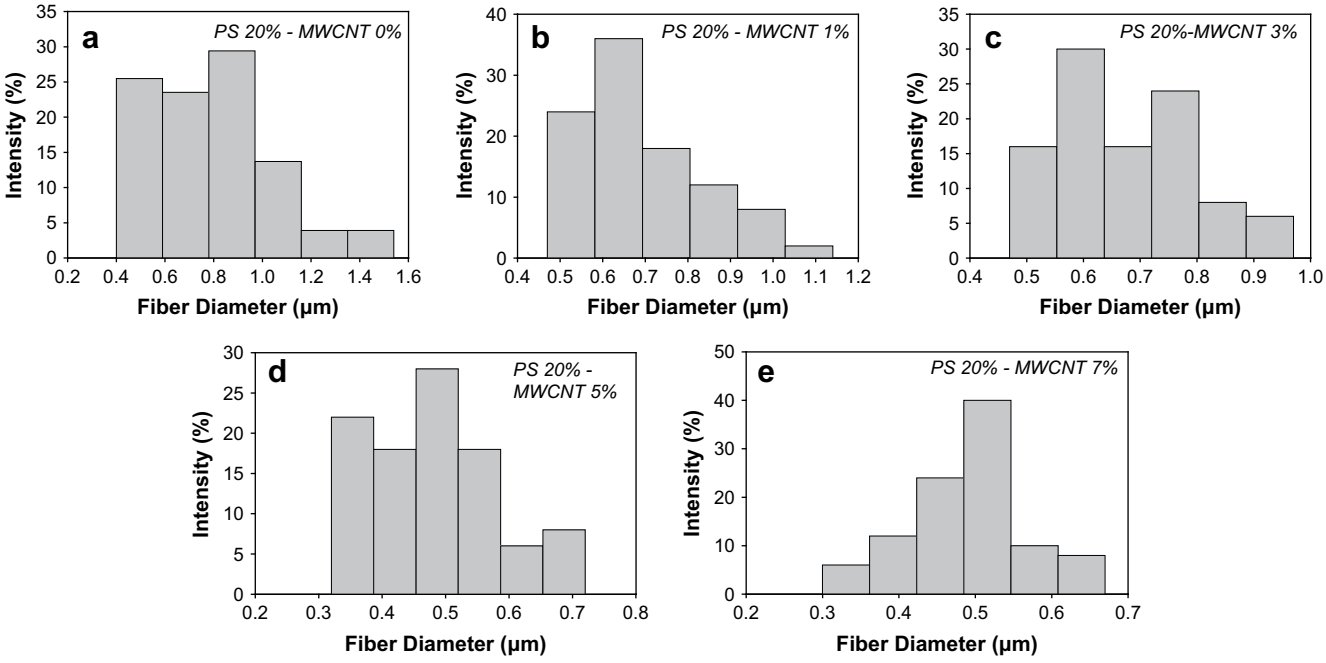

Fig. 7. Histograms of fiber diameter distribution. a) Pure PS (Average fiber diameter (R_{avg}): 766 ± 288 nm); b) 1% MWCNT (R_{avg}: 676 ± 186 nm); c) 3% MWCNT (R_{avg}: 665 ± 117 nm); d) 5% MWCNT (R_{avg}: 482 ± 83 nm); e) 7% MWCNT (R_{avg}: 518 ± 69 nm).

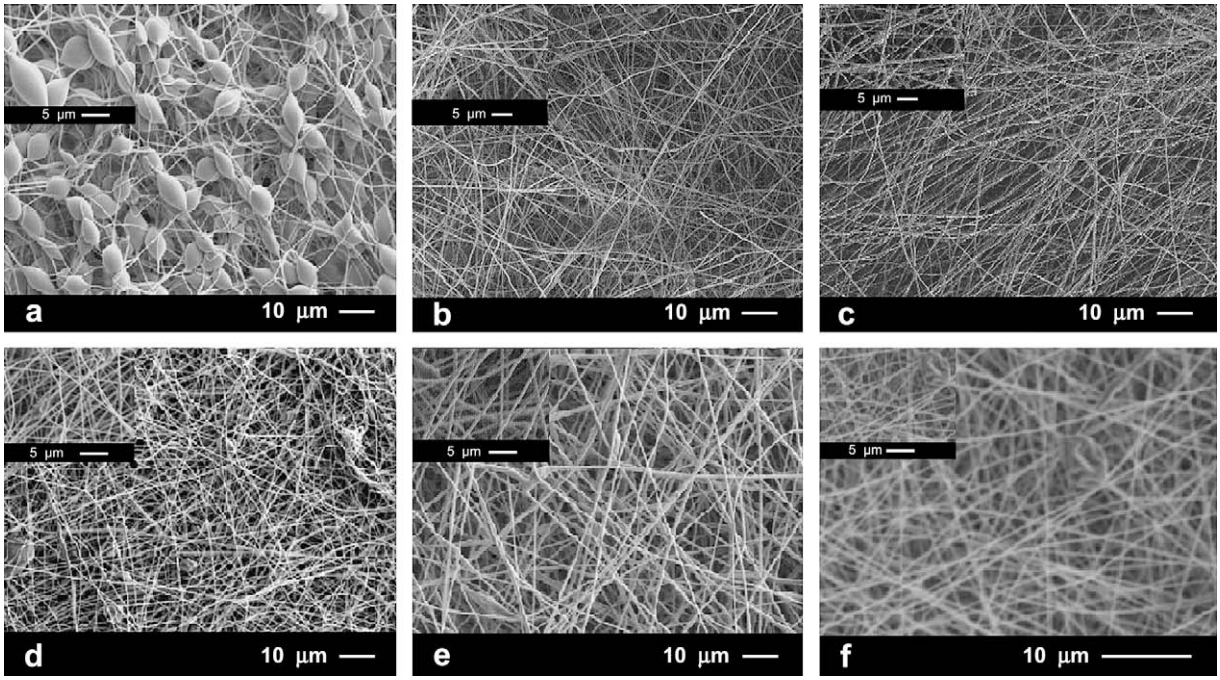

Fig. 8. SEM photos of PS (20%)/Copolymer/MWCNT at different CNT concentrations. a) Pure PS; b) 1% MWCNT, 1% Copolymer; c) 2% MWCNT, 2% Copolymer; d) 3% MWCNT, 3% Copolymer; e) 4% MWCNT, 4% Copolymer; f) 5% MWCNT, 5% Copolymer.

Fibers obtained were more uniformed in fiber diameter in this case and the range of fiber diameter does not change considerably by adding carbon nanotube concentration (Fig. 9).

The average diameter of fibers at other concentrations is even lower in samples with copolymer compared to pure MWCNT samples (Figs. 7 and 9). This is an additional proof that homogenous dispersion and electrical conduction through fibers result in a larger fiber diameter reduction. At 5% MWCNT/copolymer, the finest fibers are obtained with quite narrow fiber diameter distribution compared to other concentrations.

Optical microscopy was used in parallel with SEM to detect CNT localization inside the fibers. The samples for optical microscopy were electrospun at the processing conditions mentioned above; with the difference that a rotating drum with the speed of 120 rpm was used as collector instead of static drum to produce a thinner electrospun mat in stable electrospinning condition. Fig. 10 shows the optical images of electrospun fibers containing different concentrations of MWCNT in suspensions with and without copolymer. The results obtained from this method show that in most cases, beads in MWCNT-containing sections are filled with MWCNT agglomerates (Fig. 10). It is also possible to detect some MWCNT aggregates inside fibers; however, the large ones are located inside the beads along the fibers. At 5%, the number of bead structures increase and they are filled with MWCNTs. Even though, the fiber diameter and beads sizes decrease, most of those small beads all contain MWCNTs (Fig. 10c).

The same results were obtained from optical microscopy of the samples with both MWCNT and copolymer (Fig. 10d–f). At 1%, it was difficult to detect MWCNTs by optical microscopy. In samples containing copolymer, it shows that the sizes of MWCNT agglomerates have considerably reduced (Fig. 10d). At 3% and 5%, the fiber diameter decreased significantly; however, the bead structures are still MWCNT aggregate locations. The compatibilizing effect of copolymer has decreased the size of the beads and MWCNT aggregates along fiber axis (Fig. 10e and f).

Comparing the results of SEM and optical microscopy shows that there are two main parameters controlling the morphology of fibers for this system during electrospinning: solution conductivity and CNT dispersion condition. Increasing conductivity removes the bead structures, therefore at 1% and 2% (below carbon nanotube network formation), there are less bead structures compared to 0% and 0.5% MWCNT. Above percolation, the morphology of fibers is controlled not only by the conductivity but also by the CNT dispersion condition. At these higher concentration levels, there is

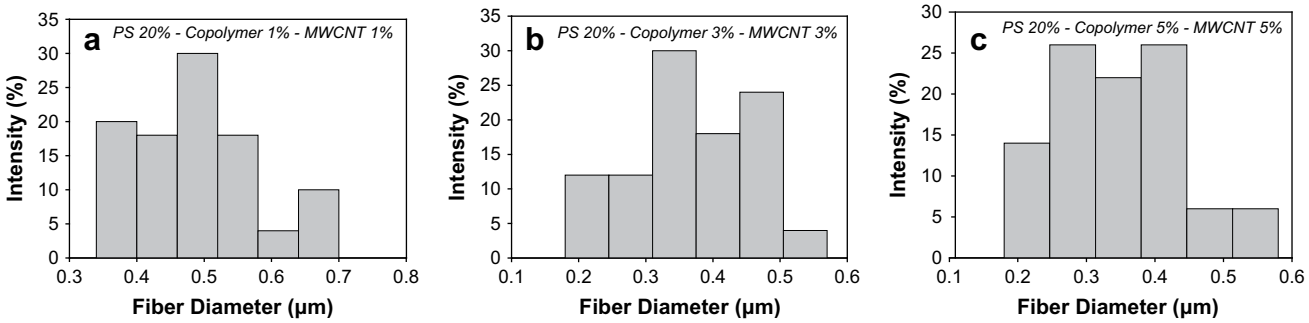

Fig. 9. Histograms of fiber diameter distribution. a) 1% MWCNT, 1% Copolymer (R_{avg}: 486 ± 108 nm); b) 3% MWCNT, 3% Copolymer (R_{avg}: 324 ± 84 nm); c) 5% MWCNT, 5% Copolymer (R_{avg}: 298 ± 105 nm).

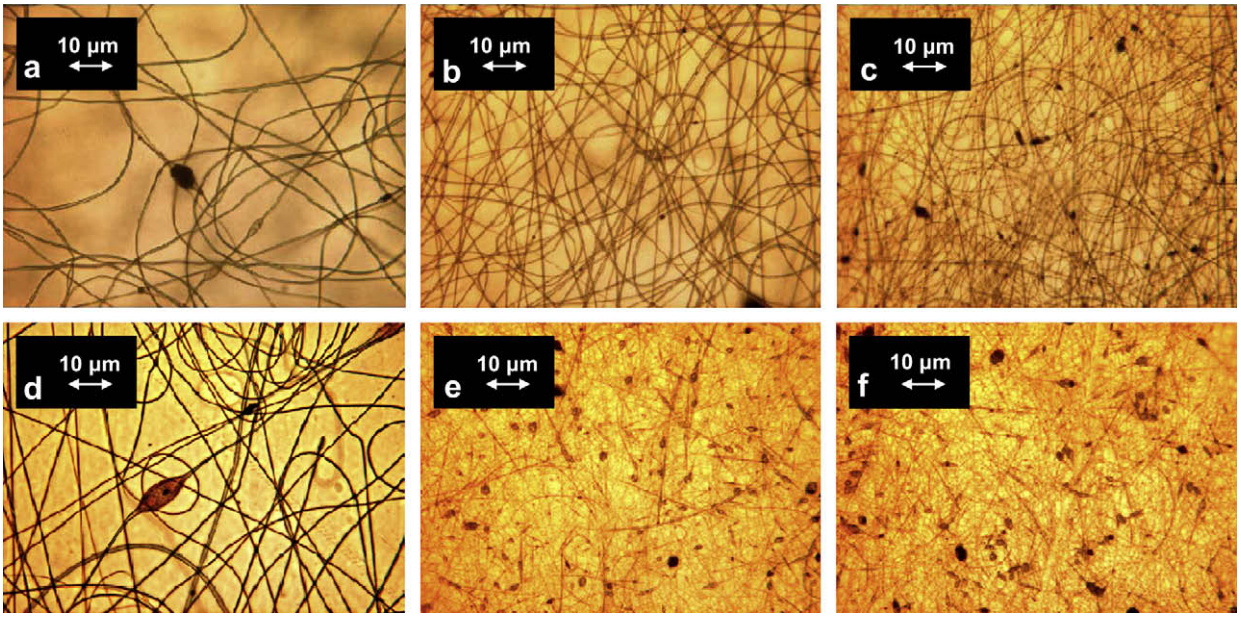

Fig. 10. Optical microscopy photos of PS/MWCNT electrospun fibers obtained at the same condition, a) 1% MWCNT; b) 3% MWCNT; c) 5% MWCNT; d) 1% MWCNT, 1% Copolymer; e) 3% MWCNT, 3% Copolymer; f) 5% MWCNT, 5% Copolymer.

no change in solution conductivity and dispersion of CNTs becomes more difficult. The dispersion condition is the controlling parameter of final fiber morphology and of bead formations. Hence, at 5% and 7% MWCNTs, the bead structure greatly increases along fiber axis which could be the result of CNTs poor dispersion. Even though, the solutions at 5% and 7% MWCNTs are in a suitable solution conductivity range to give smooth fibers (The conductivity of solution containing 5% or 7% MWCNT is more than 1% MWCNT concentration which gives quite smooth fibers), the aggregates of CNTs cause bead structures development. The same results were obtained for the samples containing copolymer, and only CNT aggregates and beads dimensions were smaller. Therefore, CNTs are better distributed with finer particles along fiber axis.

The fibers' morphology at 1% of single-wall, double-wall (below percolation threshold) as well as at 5% (above percolation threshold) are shown on Fig. 11. The systems containing SWCNT and DWCNT are mixtures of beads and fibers together. At 1% DWCNT or SWCNT (Fig. 11a and b), the amount of beads increased compared to 1% MWCNT but they still have fewer beads compared to pure PS fibers.

Quantitative analysis of SWCNT and DWCNT nanocomposite fibers shows that they both have average fiber diameters larger than those obtained for pure PS electrospun system below

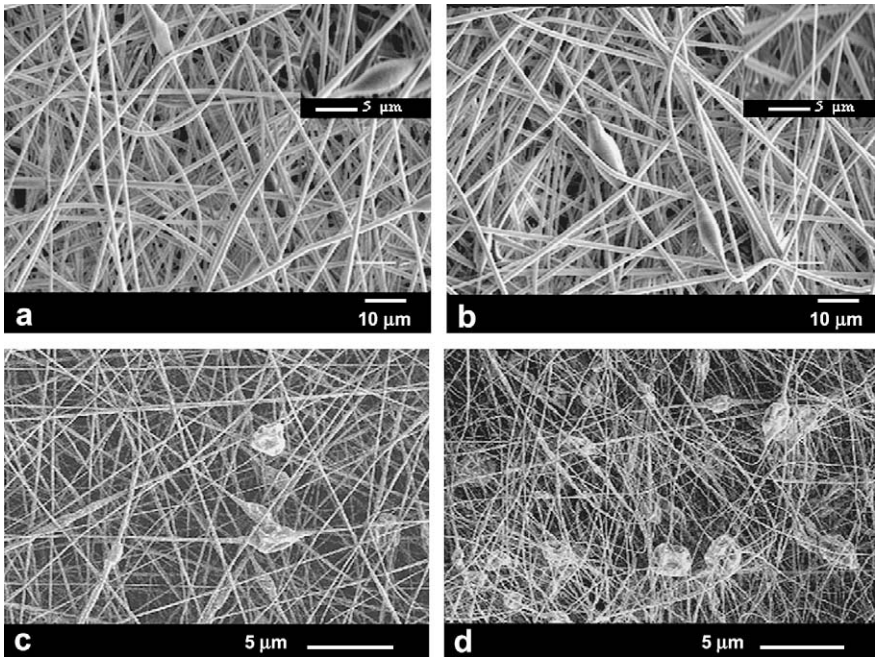

Fig. 11. SEM photos of 20% PS electrospun fiber containing a) 1% DWCNT; b) 1% SWCNT; c) 5% DWCNT; d) 5% SWCNT.

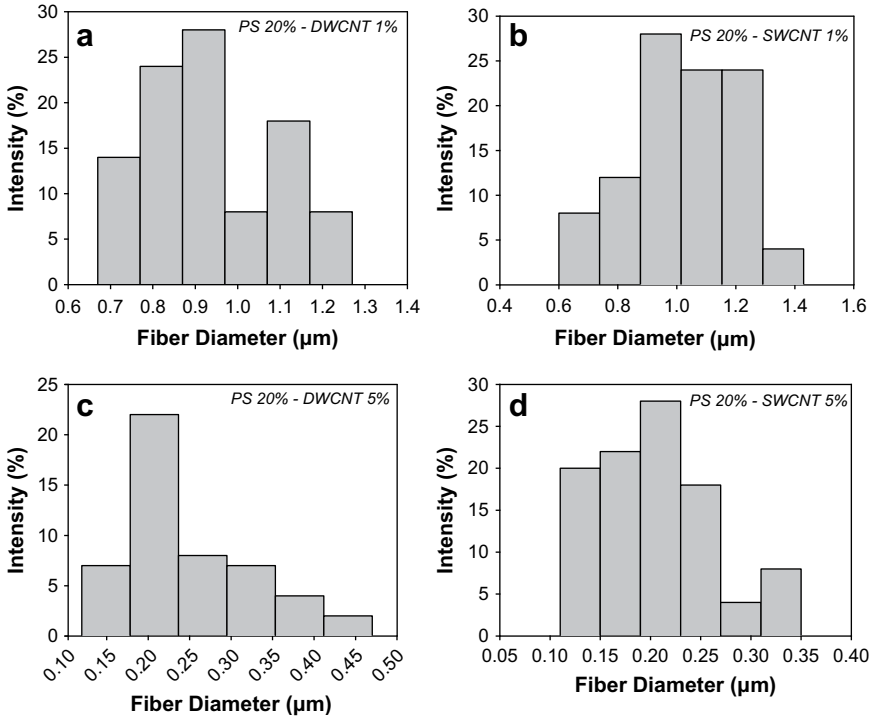

Fig. 12. Histograms of fiber diameter distribution. a) 1% DWCNT; b) 1% SWCNT; c) 5% DWCNT; d) 5% SWCNT.

percolation (Fig. 12a and b). The expectations were to observe smaller diameters because of higher conductivity of SWCNT and DWCNT, but the result is opposite. This may be due to the poor dispersion condition of SWCNT and DWCNT proved by both viscometry and optical microscopy as discussed above. The fibers show a wide diameter distribution and they are mostly located at high range of diameters. Fig. 11 also shows the morphologies of fibers at 5% of different CNTs. Fine fibers were obtained at this concentration, with few beads for DWCNT and many beads for SWCNT (Fig. 11c and d). Fibers have low diameters and they obey a normal distribution especially with SWCNT system (Fig. 12d). High conductivity of initial solution decreases the average fiber diameter; however, the fibers are mixed with many beads along axis which is the result of poor dispersion of CNTs (Fig. 12d).

Fig. 13 compares the average fiber diameter of different systems with CNTs at two concentrations. The behavior of the different systems is totally different below percolation (1% CNT) and above percolation (5% CNT). This again emphasizes the effect of the conductivity of the solution and dispersion of CNT as the parameters controlling the fiber diameter as well as morphology of electrospun fibers.

Fig. 14 briefly reviews the morphological observations obtained here at different concentrations of CNTs. As it was discussed so far, dispersion condition could be introduced as a controlling factor of final fiber morphology. In the case of good dispersion and very low concentrations of CNTs, finer fibers besides removing bead structure are expected because of increasing conductivity [6,24]. Therefore, increasing CNT concentrations decreases both bead structures and fiber diameter in all concentrations resulting from high conductivity; however, two different areas are distinguished in the case of poor dispersion based on CNT concentration and percolation threshold (Fig. 14).

The results show that both fiber diameter and smoothness could be controlled by CNT dispersion condition depending on CNT concentration. As it is depicted, at low CNTs concentrations, fibers with larger diameter are the effect of poor dispersion; while the same factor translate by larger fraction of beaded fibers at high concentrations. At low CNT concentrations, an increase in fiber diameter is observed, which is unexpected in solutions with higher conductivity compared to pure PS system due to CNT addition. It is opposite to previous observations with MWCNT dispersions since the increase in conductivity results in fiber diameter reduction [6]. Moreover, the beads disappear from the fibers at low CNT concentrations while the results show the samples have lower viscosities in

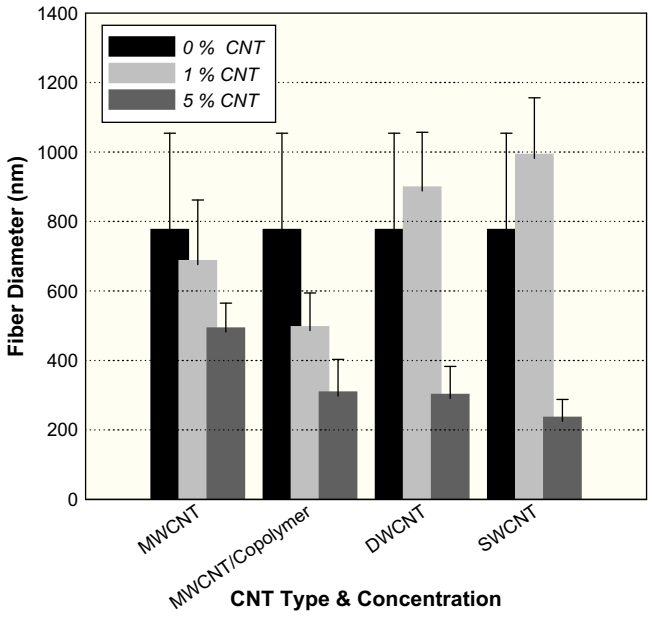

Fig. 13. Comparison of average fiber diameter at different types of CNTs below percolation (1%) and after percolation (5%).

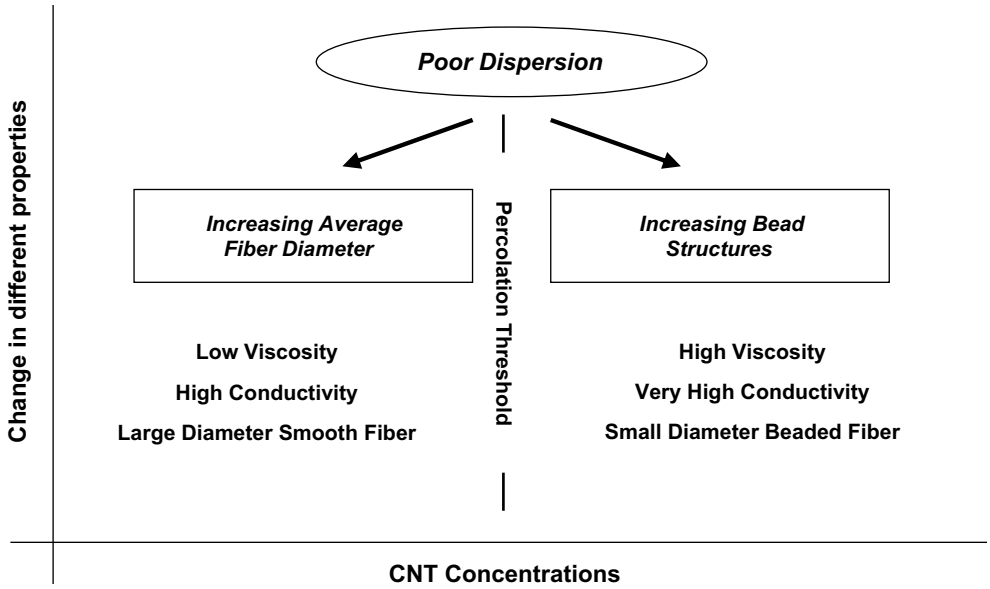

Fig. 14. The schematic diagram of change in various properties as a function of CNT concentrations and the effect of poor dispersion condition as a controlling factor.

this range. This result is opposite to previous observations for the effect of viscosity on smooth fibers formation; since the increase in viscosity was accounted as a parameter for smoother fiber formation [24]. Beads removal could be due to the increase of conductivity compared to pure electrospun nanofibers in spite of the lower viscosities of initial solution. Higher conductivity of solution is expected by adding more CNT to the system; however, an increase in fiber diameter is observed here even in highly conductive solutions especially when there is poor dispersion of CNTs (SWCNT and DWCNT). Therefore, dispersion condition is one of the controlling factors for fiber diameter besides fiber smoothness. Above percolation, the increase in conductivity and viscosity results in significant fiber diameter reduction compared to lower CNT concentrations. At higher CNT concentrations (above electrical percolation), dispersion affects final fiber morphology from another aspect. There are unexpected bead structures along fiber axis which contain CNT aggregated (Fig. 10). Poor dispersion above percolation and inhomogeneous electrical conduction along the fiber causes CNT agglomeration and bead formation. The poorer the dispersion, the more the beads are present along the fibers, while the opposite is expected at high values of viscosity and conductivity.

In summary, reduction in molecular weight and viscosity after sonication is not consistent with bead removal from fiber axis [25]; therefore other parameters except of viscosity are controlling the bead morphology and fiber diameter. Here, we believe that CNT dispersion condition and conductivity of initial solution are the main determining factors. As the results of conductivity show, addition of CNT increases the conductivity and the solutions containing SWCNT are more conductive that the solutions with coated MWCNT. Therefore, followed by increasing the initial conductivity we expect two main changes in final morphology: reduction in fiber diameter [6] and bead removal from fiber axis [22] compared to pure electrospun nanofibers. While there is an increase in fiber diameter for the samples below network formation concentration opposite to expectation (SWCNT and DWCNT) and there is increase in bead morphology by increasing the CNT concentration above network formation concentration. Increasing the fiber diameter at 1% CNT concentration in SWCNT and DWCNT which are poorly dispersed proves that dispersion condition is more important than solution conductivity in this case; while this effect is shown as bead formation at high CNT concentration. Comparing the sizes of beads obtained from optical microscopy and SEM in addition to optical microscopy results prove that all the beads are the locations of CNT aggregated and making modification on the dispersion in example by adding copolymer decreases the bead structures to a great extend.

Increasing the conductivity causes larger electric current during electrospinning and will induce large charge accumulations on fiber diameter, and as result, will intensify the electrical force and splashing and finer fibers are formed [37]. In this system, the solvent (DMF) is non-conductive compared to PS/CNT complex and the polymer (PS/CNT) is the charge carrier in these kinds of systems; since the polymer (PS/CNT) is more conductive and the conductivity of solution is dependent on CNT. Therefore, when the CNT is well dispersed, and before network formation, the charge accumulates uniformly on fiber surface and the reduction of fiber diameter along with smooth fiber formation is observed (1% MWCNT and 1% and 2% MWCNT/Copolymer). However, when CNT is not well dispersed, there is localized charge accumulation along fiber axis because of inhomogeneity of polymer solution conductivity. In this case the charge density is not dispersed uniformly along fiber and therefore electric field is not homogenous along fiber. The inhomogeneity of charges and electric field causes bead formation along fiber axis. It means that in some parts, the fiber diameter reduces and in the other parts there are bead structures and increase in fiber diameter (SWCNT and DWCNT solutions in all concentrations and MWCNT solutions above network formation concentration). In 1% SWCNT and 1% DWCNT solutions the quality of dispersion is not satisfactory; therefore beads are formed even at low concentration. However, because of lower conductivity compared to 5% CNT, the charge density and electric field are not strong enough for fiber diameter reduction. As a result, the presence of aggregated CNT causes an increase in the fiber diameter because there is not a strong electric field; moreover, the inhomogeneity of charge density induces the bead formation.

3.4. Electrical conductivity results of fiber mats

Electrical conductivity of final electrospun mat was measured as a function of CNT type and concentration. The samples included a wide range of thicknesses from 15 to 300 μm and they were all positioned between two highly conductive layers besides electrodes

before starting experiments. The conductivities of all samples were measured in a specific two-probe test fixture. Therefore, all the experiments were run in similar conditions, constant force and with reliably enough repeatability within 80% of the average conductivity.

Based on electrical percolation theory, the system becomes conductive when a critical concentration is reached which is called percolation threshold. Above electrical percolation, the system is quite conductive. Formation of CNT network causes the electron transport by tunneling or electron hopping which occurs along CNT interconnects [38]. The system studied was the 20% PS and was below percolation for CNTs content up to 2%. No network structure or CNT agglomerate is formed up to 2% MWCNT, which was shown before by viscometry and optical microscopy of initial solution. In MWCNT concentrations above 2%, an internal network structure is formed and the system is getting close to percolation. Below 3% our instrument and set-up was not showing any results which could depict considerable electrical conductivity in the system. At 3% MWCNT and above, sensible modification in conductivity of PS electrospun mat was observed from electrical conductivity measurements. However, 3% MWCNT is not enough to form complete network and to achieve the electrical percolation threshold and the samples are still in the transition region to percolation (1.90×10^{-9} S/cm). Therefore, the conductivity of non-woven mat at 1% and 2% MWCNT concentration is almost zero (Between 10^{-19} and 10^{-9} (PS/3%MWCNT)). At 3.5% concentration of MWCNT, samples are at electrical percolation threshold (1.02×10^{-5} S/cm) and a considerable increase in electrical conductivity is observed after this concentration (Fig. 15). At 5% and 7% CNTs, the conductivity increased; however, the value of conductivity was almost constant after 5% MWCNT (Fig. 15). This confirms the results obtained from viscometry which indicate the start of network formation above 2% MWCNT. At 3% the sample is at the beginning of the construction of a complete network, and at 3.5% CNT concentration, the network is complete resulting in a totally conductive mat. Based on percolation theory [39]:

$$\sigma = A(w - w_c)^t \quad (1)$$

where σ is the volume conductivity, A and t are constants, and w_c is the critical concentration in which the conductivity is ignorable compared to higher concentration; the critical concentration for network formation. Considering 3% as w_c, we could obtain $A = 8.5 \times 10^{-5}$ and $t = 0.795$ for this system. We have measured the conductivity through the thickness of non-woven mat. It means that at 3.5% MWCNT, there are networks for electron transfer between the layers of non-woven mat based on percolation theory. Therefore, the random structures of fibers, which are making different layers of non-woven mat, have enough CNT to make network between layers. As a result, it is possible to predict that the value of conductivity would be more and the percolation threshold would be less even if the conductivity is measured along fiber axis.

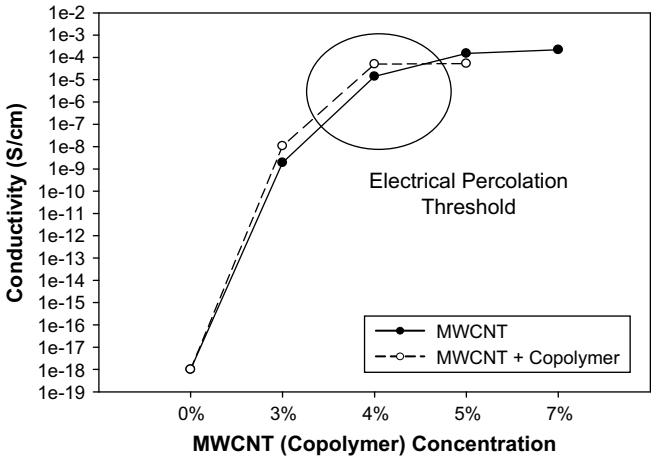

Fig. 15. Conductivity of samples containing copolymer comparing to samples without copolymer.

For the samples containing both MWCNT and copolymer, a similar concentration effect on the electrical conductivity was found. The electrical percolation threshold (5×10^{-5} S/cm) was observed for 4% CNT concentration. The results obtained show that the electrical conductivity of mats containing compatibilizer is slightly higher than samples containing MWCNT without compatibilizer, below and around percolation threshold (Fig. 15). The higher values of conductivity originate probably from the good dispersion condition of MWCNTs in the samples, which reduces agglomeration and helps distribution of MWCNTs along fiber axis. Improving dispersion helps in conductivity modification below percolation. However, after percolation (5%), a decrease in conductivity of sample containing copolymer is observed compared to only MWCNTs containing samples (Fig. 15). Moreover, the conductivity reached a constant value more rapidly in samples with copolymer. This might be the result of a reasonable dispersion of CNTs around percolation.

Good dispersion is expected to increase conductivity of mats compared to samples without copolymer. However, coating and compatibilization above percolation may have a reverse effect on conductivity. At 5% w/w concentration, the network of CNTs is organized in the sample with both copolymer and pure MWCNT. Addition of copolymer partially coats the MWCNTs and therefore in spite of forming networks; it could reduce the electrical conduction as has been previously observed [8].

The conductivities of samples with 5% SWCNT and 5% DWCNT were also measured. At this content, SWCNT shows the highest conductivity as expected (3.7×10^{-4} S/cm). The samples with MWCNT/Copolymer (5.3×10^{-5} S/cm) and DWCNT (5.0×10^{-5} S/cm) show the lowest amount of electrical conductivity. It should be noted that, however, it is quite difficult to disperse the samples with SWCNT and DWCNT, and the fibers obtained show the presence of CNT aggregates in the fibers in addition to the beads structure. However, the unique structure of SWCNT overcomes the poor dispersion of CNTs and the best conductivity is obtained.

3.5. Mechanical characterization of fiber mats

Electrospun PS/MWCNT fiber mats were studied in both cases of with and without compatibilizing copolymer. For the samples without copolymer, addition of MWCNT causes an increase in both modulus and tensile strength before percolation threshold (Fig. 16). A gradual increase is observed up to 2% CNT; then a jump in modulus and tensile strength is observed at 3% MWCNT. Above 3% MWCNT, modulus and tensile strength decrease and they are even less than pure PS at 5% MWCNT. At 4% MWCNT, the internal network of CNT is formed and it is thought to be the main reason for weakening of nanocomposite mats. Since the formation of network is accompanied with weakening of CNT/matrix at high concentrations of CNTs. Increasing MWCNT content and network formation decreases the strength of final PS mat and a reduction in mechanical properties is obtained. The materials obtained above percolation are quite brittle and weak (Fig. 16). Almost the same behavior was observed for maximum tensile strain (ε_{max}) in the samples containing MWCNT (Fig. 16). The increase of modulus at all concentrations of MWCNT below percolation causes a change into brittle behavior and accordingly, causes a decrease in ε_{max} compared to pure PS. The value of ε_{max} in all concentrations is less than pure PS non-woven mat.

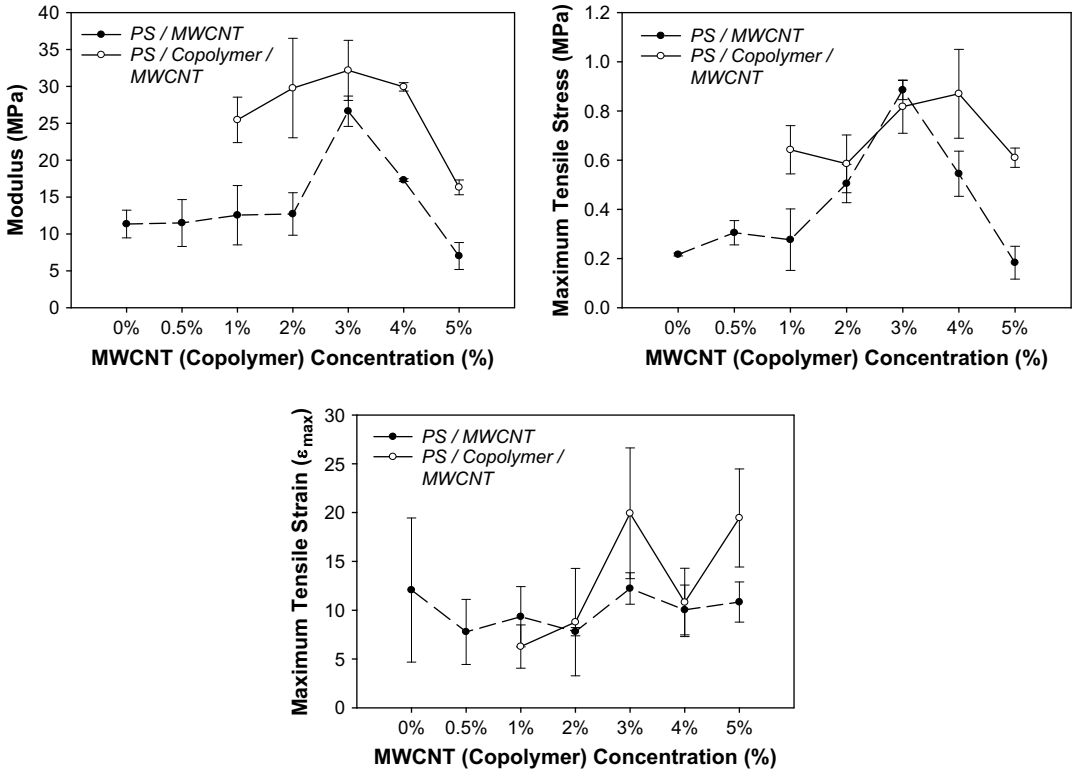

Fig. 16. Tensile modulus, maximum tensile stress and maximum tensile strain as a function of MWCNT concentrations with and without copolymer.

A comparison of the values of modulus and tensile strength with those of the samples containing only MWCNT shows a significant copolymer effect. The modulus and tensile strength are about twice for the samples containing copolymer (Fig. 16). Only at 3% MWCNT the value of tensile strength in both samples with and without copolymer is almost the same. Moreover, above percolation, improved mechanical properties for samples containing MWCNT and copolymer are still observed compared to pure PS. Therefore, not only quite conductive systems are obtained above electrical percolation, but also improved mechanical properties are achieved. The behavior of maximum tensile strain (ε_{max}) for the samples with MWCNT and copolymer is totally different from pure MWCNT nanocomposite fibers. ε_{max} increases as a function of MWCNT concentration and it does not decrease even after percolation at 5% MWCNT/Copolymer concentration (Fig. 16). It is to be reminded here that any increase in MWCNT is accompanied with the same increase in copolymer concentration for compatibilised nanocomposites. Therefore, copolymer addition brings tough behavior to the electrospun mats even with addition of MWCNT and decreasing modulus after percolation.

The localization of the compatibilizer at the interface of CNT and polymer matrix improves the mechanical strength [40]. The results obtained from the mechanical tests and increasing in ε_{max} prove that the added copolymers are improving the interactions at the interface. The improved interface due to copolymer addition results in better mechanical strength of final nanocomposite electrospun mats. From another point of view, addition of copolymer might cause developing a kind of PS/SBS blend as the matrix. The formation of the blend by adding copolymer concentration causes tough behavior of the system and increase in ε_{max}.

The effect of different types of CNTs on final mechanical properties was also studied (Table 4). As shown, in contrast with electrical conductivity results, DWCNT shows the best mechanical properties' results. The highest values of modulus, tensile strength and ε_{max} were obtained for the samples with DWCNT. This might originate from the small size of DWCNT compared to MWCNT and more interface and connection with matrix. Compared to SWCNT, DWCNT is easier to disperse and therefore, the mechanical test results improve by adding DWCNT. In the case of SWCNT, in spite of the small sizes of nanotubes, poor dispersion causes the mechanical properties to deteriorate. Similar results have been obtained previously in literature on the effect of DWCNT in mechanical properties modification and obtaining better results compared to MWCNT and SWCNT [34].

Samples containing both MWCNT and copolymer show best improvement in both mechanical and electrical properties (above percolation). Therefore, the compatibilised MWCNT samples could give the best results from different aspects of view and this is of great interests.

Table 4
Mechanical properties of different CNT types.

CNT type	Modulus (MPa)	Maximum tensile stress (MPa)	Maximum elongation (ε_{max})
5% MWCNT	7.0 ± 1.8	0.18 ± 0.07	10.8 ± 2
5% MWCNT/copolymer	16.3 ± 0.1	0.61 ± 0.04	19.4 ± 5
5% SWCNT	10.4 ± 2.0	0.22 ± 0.05	8.6 ± 5
5% DWCNT	23.4 ± 8.6	0.78 ± 0.16	12.3 ± 1

4. Conclusions

PS nanocomposite nanofibers combined with different types of CNTs were electrospun in this work for the first time. The final structures and morphologies of electrospun nanocomposite nanofibers were studied along with electrical and mechanical properties of resulting mats. A copolymer was used to improve the dispersion condition of CNT and the resulting suspension was analyzed by means of optical microscopy and viscometry. Comparison of the final morphologies of samples with different dispersion conditions showed that CNT dispersion is an important controlling parameter

for final fibers diameter and morphology. Below percolation, poorly dispersed samples showed an unexpected increase in fiber diameter while above percolation threshold, beads formation resulted from poor nanoparticles dispersion. Reasonable electrical conductivity was obtained at the percolation threshold of 4% MWCNT. Electrical conductivity results proved the positive effect of copolymer addition below percolation threshold. However, above percolation, the samples with copolymer showed a lower conductivity which might be because of CNTs coating with copolymer. Moreover, morphologies and final properties of electrospun fibers with different types of CNTs (SWCNT, DWCNT, MWCNT, and compatibilised MWCNT) at different concentrations and percolation region were compared in this work. The results show the important effect of dispersion on final fiber morphologies and properties. The best conductivity obtained in SWCNT/PS mixture in spite of poor dispersion. While adding copolymer causes better conductivity results below percolation in MWCNT/PS mixture. The effect of copolymer on improved compatibility was proved through comparison of the mechanical properties test results between PS/MWCNT and PS/Copolymer/MWCNT systems.

Acknowledgement

The authors would like to acknowledge the financial support of Natural Sciences and Engineering Research Council Canada (NSERC) and from FQRNT (Fonds Québécois de Recherche en Nature et Technologies) for the financial support to carry out this study.

References

[1] Burger C, Hsiao BS, Chu B. Annual Review of Materials Research 2006;36:333–68.
[2] Li D, Xia Y. Advanced Materials 2004;16(14):1151–70.
[3] Reneker DH, Chun I. Nanotechnology 1996;7(3):216–23.
[4] Iijima S. Nature 1991;354(6348):56.
[5] Ge JJ, Hou H, Li Q, Graham MJ, Greiner A, Reneker DH, et al. Journal of the American Chemical Society 2004;126(48):15754–61.
[6] Ra EJ, An KH, Kim KK, Jeong SY, Lee YH. Chemical Physics Letters 2005;413(1–3):188–93.
[7] Seoul C, Kim YT, Baek CK. Journal of Polymer Science, Part B: Polymer Physics 2003;41(13):1572–7.
[8] Sung JH, Kim HS, Jin HJ, Choi HJ, Chin IJ. Macromolecules 2004;37(26):9899–902.
[9] Dror Y, Salalha W, Khalfin RL, Cohen Y, Yarin AL, Zussman E. Langmuir 2003;19(17):7012–20.
[10] Dror Y, Salalha W, Pyckhout-Hintzen W, Yarin AL, Zussman E, Cohen Y. Progress in Colloid & Polymer Science 2005;130:64–9.
[11] Salalha W, Dror Y, Khalfin RL, Cohen Y, Yarin AL, Zussman E. Langmuir 2004;20(22):9852–5.
[12] Delozier DM, Watson KA, Smith Jr JG, Clancy TC, Connell JW. Macromolecules 2006;39(5):1731–9.
[13] Nativ-Roth E, Shvartzman-Cohen R, Bounioux C, Florent M, Dongsheng Z, Szleifer I, et al. Macromolecules 2007;40(10):3676–85.
[14] Sluzarenko N, Heurtefeu B, Maugey M, Zakri C, Poulin P, Lecommandoux S. Carbon 2006;44(15):3207–12.
[15] Casper CL, Stephens JS, Chase DB, Rabolt JF. Polymer Preprints (American Chemical Society, Division of Polymer Chemistry) 2003;44(2):81.
[16] Jarusuwannapoom T, Hongrojjanawiwat W, Jitjaicham S, Wannatong L, Nithitanakul M, Pattamaprom C, et al. European Polymer Journal 2005;41(3):409–21.
[17] Kang M, Yoon SH, Jin HJ. Polymer Preprints (American Chemical Society, Division of Polymer Chemistry) 2005;46(2):812–3.
[18] Lee KH, Kim HY, Bang HJ, Jung YH, Lee SG. Polymer 2003;44(14):4029–34.
[19] Megelski S, Stephens JS, Rabolt JF, Bruce Chase D. Macromolecules 2002;35(22):8456–66.
[20] Pattamaprom C, Hongrojjanawiwat W, Koombhongse P, Supaphol P, Jarusuwannapoo T, Rangkupan R. Macromolecular Materials and Engineering 2006;291(7):840–7.
[21] Wannatong L, Sirivat A, Supaphol P. Polymer International 2004;53(11):1851–9.
[22] Uyar T, Besenbacher F. Polymer 2008;49(24):5336–43.
[23] Lin T, Wang H, Wang H, Wang X. Nanotechnology 2004;15(9):1375–81.
[24] Shenoy SL, Bates WD, Frisch HL, Wnek GE. Polymer 2005;46(10):3372–84.
[25] Eda G, Shivkumar S. Journal of Materials Science 2006;41(17):5704–8.
[26] Eda G, Shivkumar S. Annual technical conference – ANTEC, Conference Proceedings 2006. Charlotte, NC, United States: Society of Plastics Engineers, Brookfield, CT 06804–0403, United States.
[27] Shivkumar S, Eda G, James L. Materials Letters 2007;61(7):1451–5.
[28] Wang C, Hsu CH, Lin JH. Macromolecules 2006;39(22):7662–72.
[29] Sen R, Bin Z, Perea D, Itkis ME, Hui H, Love J, et al. Nano Letters 2004;4(3):459–64.
[30] Yuan Ji SG, Koo J, Li B. MAR06 Meeting of The American Physical Society, 2006.
[31] Pan C, Ge LQ, Gu ZZ. Composites Science and Technology 2007;67(15–16):3271–7.
[32] Sundaray B, Subramanian V, Natarajan TS. Journal of Nanoscience and Nanotechnology 2007;7:1793–5.
[33] Coleman JN, Khan U, Blau WJ, Gun'ko YK. Carbon 2006;44(9):1624–52.
[34] Gojny FH, Wichmann MHG, Fiedler B, Schulte K. Composites Science and Technology 2005;65(15–16):2300–13.
[35] Antunes EF, Lobo AO, Corat EJ, Trava-Airoldi VJ. Carbon 2007;45(5):913–21.
[36] Corrias M, Serp P, Kalck P, Dechambre G, Lacout JL, Castiglioni C, et al. Carbon 2003;41(12):2361–7.
[37] Fridrikh SV, Yu JH, Brenner MP, Rutledge GC. Physical Review Letters 2003;90(14):144502.
[38] Kota AK, Cipriano BH, Duesterberg MK, Gershon AL, Powell D, Raghavan SR, et al. Macromolecules 2007;40(20):7400–6.
[39] Wang Q, Dai J, Li W, Wei Z, Jiang J. Composites Science and Technology 2008;68(7–8):1644–8.
[40] Ye H, Lam H, Titchenal N, Gogotsi Y, Ko F. Applied Physics Letters 2004;85(10):1775–7.